

Voltage and Reactive Power Combined Control of Utility Devices and Smart Inverters on a Distribution Grid with Solar PV

Steven B. Poore
SPARK Lab, Pigman Eng. College
University of Kentucky
Lexington, KY, USA
stevenpoore@uky.edu

Rosemary E. Alden
SPARK Lab, Pigman Eng. College
University of Kentucky
Lexington, KY, USA
rosemary.alden@uky.edu

Evan S. Jones
Dept. of Electronic & Electrical Eng.
Duke Energy
Charlotte, NC, USA
sevanjones@outlook.com

Thomas Morstyn
Dept. of Engineering Science
University of Oxford
Oxford, United Kingdom
thomas.morstyn@eng.ox.ac.uk

Aron Patrick
alpatrick@pplweb.com
PPL Corporation
Allentown, PA, USA
thomas.morstyn@eng.ox.ac.uk

Dan M. Ionel
SPARK Lab, Pigman Eng. College
University of Kentucky
Lexington, KY, USA
dan.ionel@ieee.org

Abstract—With adoption of distributed energy resources (DERs) expected in future grids, voltage regulation methods need to be reevaluated and improved to ensure their effectiveness under the high volatility of renewable generation. A multi-timescale cluster-based method is proposed to optimize and disperse operation of voltage controlling utility devices including capacitor banks (CBs) and load tap changers (LTCs) while allowing faster response time with customer-owned smart inverters (SIs) in-between switching operations. The proposed method is tested on a digital twin (DT) of a very large utility distribution grid with 2,018 nodes and 8.65MW peak load to evaluate its effectiveness in future grid conditions with high DER penetration. The proposed method reduced the total energy by 1.66%, in the projected range of conservation voltage reduction (CVR), while limiting CB and LTC switching operations to 35 and 7 total adjustments respectively over a 24-hour period.

Index Terms—Volt/var control (VVC), smart inverter (SI), solar PV, electric vehicle (EV), distribution grid

I. INTRODUCTION

Increased renewable generation in future distribution grids, especially solar PV, may introduce new challenges and opportunities related to control and management. A high resistance-to-reactance ratio is a common characteristic of distribution grids, making system voltage very sensitive to active power injections [1]. To maintain compliance within the acceptable voltage range, utilities operate voltage controlling devices such as capacitor banks (CBs), load tap changers (LTCs), and voltage regulators (VRs). High volatility of renewable generation could make future distribution grids more susceptible to voltage instability, thus historical voltage control methods may need to be improved [2].

Adoption of smart inverter (SI) technology could help mitigate voltage instability in future distribution grids with high solar PV penetration. The IEEE 1547 standard, which

provides technical specifications for connection of distributed energy resources (DERs) in utility distribution systems, states that SIs should provide voltage support by injecting/absorbing reactive power during over/under voltage conditions [3]. This function is known as volt/var control (VVC) and performed by SIs with dynamic power factor (PF) capabilities [4].

In literature, some authors employed deep learning methods to maintain system voltage by optimizing VVC of SIs [5], [6]. One study proposed a multi-agent decentralized Markov decision framework for SIs to decrease reliance on communication and improve control response time [7]. Some studies have proposed coordination of customer-owned SIs with existing utility devices including CBs and LTCs [8], [9]. Multi-timescale operation of these devices has been proposed in literature to limit switching operations of CBs and LTCs while implementing faster responses from SIs [10], [11].

In the United States, utilities must deliver electricity to consumers within the acceptable voltage range of 0.95 to 1.05pu [12]. Conservation voltage reduction (CVR) refers to the advanced control and management of these devices. Traditionally, CVR refers to the intentional operation of system equipment to provide energy savings by reducing voltages to the lower end of the standard margin [13]. As reported by utilities, the standard energy reduction due to implementation of CVR is 1 to 4% [14].

Proposed in this study is multi-timescale combined control of SIs, LTCs, and CBs using a novel cluster-based method to disperse switching operations of utility devices while allowing fast response voltage support with SIs. The proposed method was tested on a digital twin (DT) of a real utility distribution grid with high DER penetration. Cluster-based control without SI VVC and traditional conventional control were also simulated as base or conventional operation for comparison

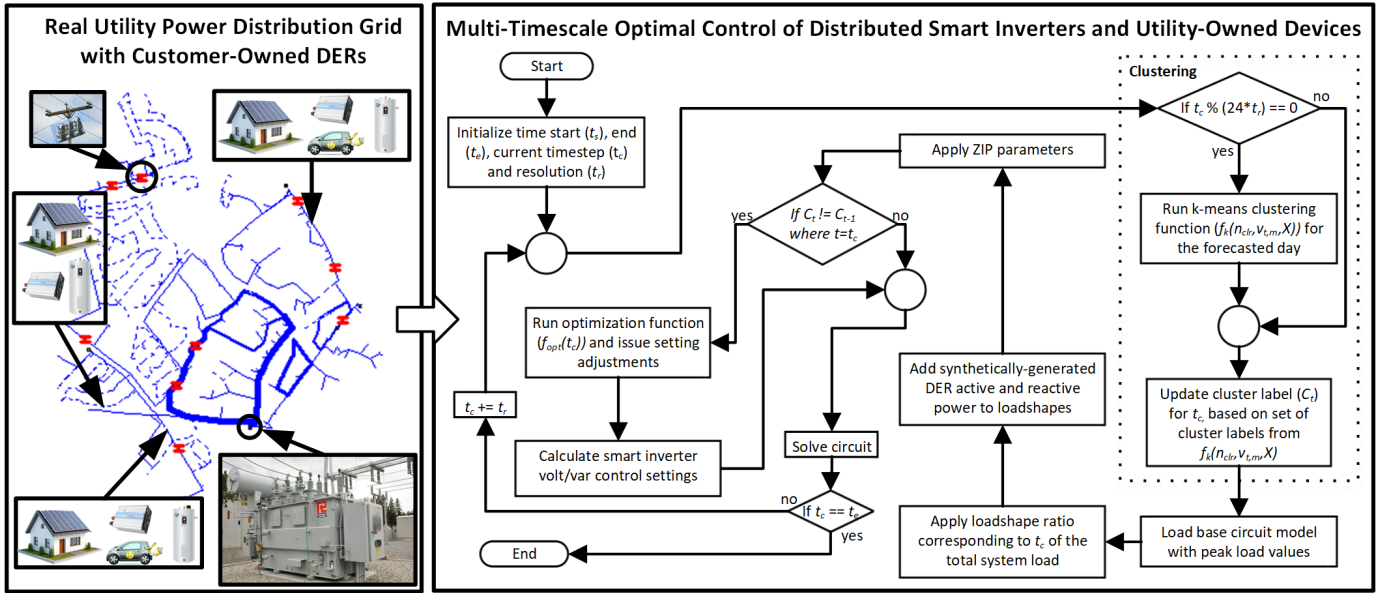


Fig. 1. The proposed cluster-based method to implement voltage and reactive power control while limiting device adjustments was simulated on a large real distribution grid equipped with nine CBs and an LTC at the substation transformer. The algorithm used to implement the proposed method is demonstrated in the flowchart above.

with the proposed method. Contributions include: voltage and reactive power optimization on a digital twin (DT) of a real, very large power distribution system with high solar PV generation; evaluation of voltage and reactive power support with vs. without SI VVC; and a multi-timescale approach for SI VVC combined with cluster-based control of LTCs and CBs to disperse operations over time while minimizing active power load and voltage violations and maximizing CVR energy reduction.

II. REAL DISTRIBUTION CIRCUIT DIGITAL TWIN AND EXPERIMENTAL DATA

The following case studies were implemented on KUS1T1, a DT of a very large real distribution grid with 8.65MW peak load, 2,018 nodes, 9 CBs, and an LTC at the substation transformer as shown in Fig. 1. The system load shape was applied using experimental power data measured at the main feeder. Constant impedance, current, and power (ZIP) load modeling was utilized to model the relationship between power and voltage as defined in [15]. A ZIP model was applied for each individual load on the circuit, and active and reactive power were defined as:

$$p = p_0 \left[a_p \left(\frac{|v|}{v_0} \right)^2 + b_p \left(\frac{|v|}{v_0} \right) + c_p \right], \quad (1)$$

$$q = q_0 \left[a_q \left(\frac{|v|}{v_0} \right)^2 + b_q \left(\frac{|v|}{v_0} \right) + c_q \right], \quad (2)$$

where p is the active power load; a_p , b_p , c_p , the first, second, and third ZIP parameters that must sum to 1; $|v|$, the voltage magnitude; v_0 , the base voltage; q , the reactive power load; and a_q , b_q , c_q , the fourth, fifth, and sixth ZIP parameters that must

also sum to one. Equivalent ZIP parameters for KUS1T1 were determined based on measurements taken from the substation transformer and each individual load model was updated to the ZIP type.

In addition to the experimental baseload measurements, thousands of synthetically-generated DER profiles were introduced to the circuit to represent a distribution grid with high DER penetration. This includes over 600 solar PV generation profiles, which were synthetically generated based on the SHINES experimental field demonstration managed by the Electric Power Research Institute (EPRI) [16]. A profile of high volatility was purposefully chosen from the dataset to simulate a worst-case voltage instability scenario. For additional PV profiles, random synthetic variation between $\pm 2\%$ was applied to the original profile to represent slight variation in generation at different physical locations within the distribution system, as shown in Fig. 2.

Electric vehicle (EV) charging and heat pump water heater (HPWH) power profiles were generated based on human behavior data from the 2017 National Household Travel Survey (NHTS) and California Building Energy Code Compliance (CBECC-Res) respectively [17], [18]. The methodology used to generate these profiles is explained in further detail in a previous publication by our group [19]. Each load on KUS1T1 was randomly assigned one HPWH profile, one EV charging profile, and one solar PV generation profile, which were added to the experimental baseload power.

III. DISPATCH OF SIs FOR VOLTAGE AND REACTIVE POWER SUPPORT

The two most common practices for dispatch of SIs are volt/watt control (VWC) and volt/var control (VVC). The

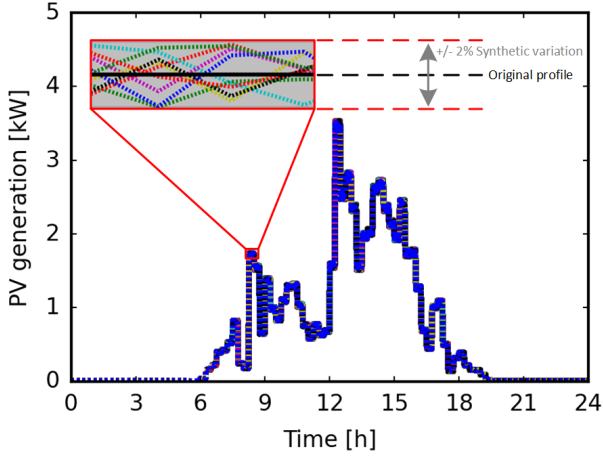


Fig. 2. A purposefully volatile experimental solar PV generation profile was selected from the SHINES dataset. Hundreds of unique profiles were derived from the original by introducing random synthetic variation of $\pm 2\%$ at each timestep.

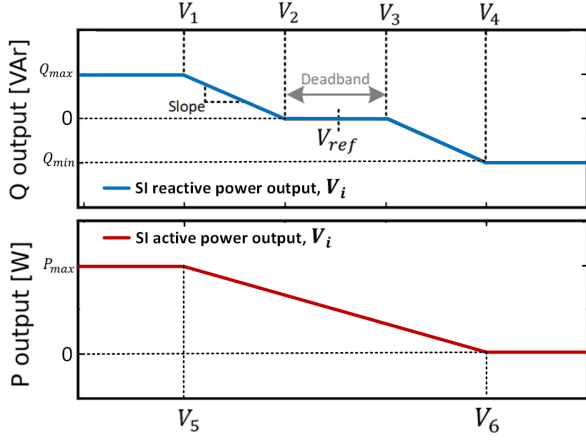


Fig. 3. Control curves for VVC (top) and VWC (bottom). To implement a combination of VVC and VWC, called volt/var/watt control (VVWC), V_4 and V_5 should be set equal to avoid curtailment of watts unless VVC alone cannot maintain voltage compliance.

control curves for VVC and VWC are illustrated in Fig. 3. For VVC, available SI capacity is used to inject/absorb reactive power to provide voltage support. If the SI capacity is oversized in comparison to the connected solar PV array, VVC control may be implemented without curtailment of active power since there would always be available capacity. The amount of reactive power to inject/absorb for SIs implementing VVC is determined by the following piecewise function:

$$Q_i(V_i) = \begin{cases} Q_{max}, & V_i < V_1 \\ \frac{Q_{max}}{V_2 - V_1}(-V_i + V_2), & V_1 < V_i < V_2 \\ 0, & V_2 < V_i < V_3 \\ \frac{Q_{min}}{V_4 - V_3}(V_i - V_2), & V_3 < V_i < V_4 \\ Q_{min}, & V_i > V_4 \end{cases} \quad (3)$$

where Q_{min} , Q_{max} are the maximum amount of reactive power that can be absorbed or injected respectively by the SI;

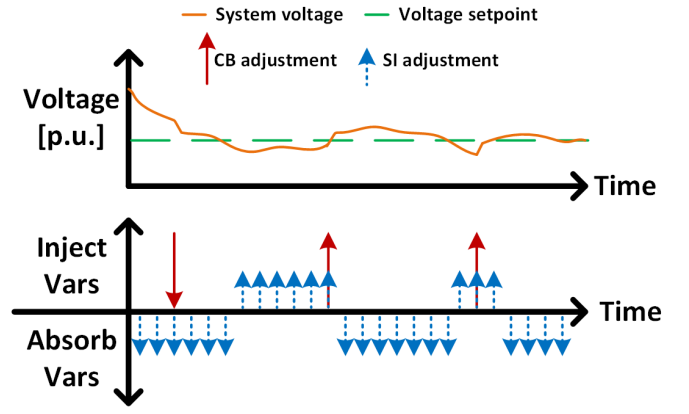


Fig. 4. The proposed method includes multi-timescale combined control of utility-owned equipment with customer-owned SIs. More frequent adjustments can be made with SIs, allowing additional reactive power support in-between CB switching operations to better maintain target CVR voltage.

V_i is the voltage measured at the point of common coupling (PCC); and V_1 , V_2 , V_3 , and V_4 are the VVC voltage setpoints.

Under VWC, SIs curtail solar PV active power output to avoid system over-voltage conditions. For distribution grids with high solar PV penetration, voltage may spike when PV output is high due to the sudden decrease in effective load, so active power may need to be curtailed in some cases. For each SI in VWC, active power output is determined by the following piecewise function:

$$P_i(V_i) = \begin{cases} P_{max}, & V_i < V_5 \\ \frac{-P_{max}}{V_6 - V_5}(V_i - V_6), & V_5 < V_i < V_6 \\ P_{min}, & V_i > V_4 \end{cases} \quad (4)$$

where P_{max} is the available capacity; V_i is the voltage measured at the PCC; and V_1 , V_2 , V_3 , and V_4 are the VVC voltage setpoints.

Additionally, the combination of VVC and VWC, called volt/var/watt control (VVWC) may be implemented. In this case, V_5 is set equal to V_4 to avoid curtailment of watts unless absolutely necessary. For the case study in section V, only VVC is considered and operable SI PF range is assumed to be 0.8 lagging to 0.8 leading, which is consistent with available SIs on the market for residential applications [20]. The capacity for each SI was assumed to be 7.65kVA, which is oversized from the 4kW solar PV arrays at each load.

IV. CLUSTER-BASED METHOD FOR VOLTAGE AND REACTIVE POWER CONTROL

A new cluster-based optimization method is used to control utility devices for the case study in section V. Utility devices typically used for voltage and reactive power control, such as CBs and LTCs, were limited in the number of adjustments executed within a given time frame to minimize degradation. A k-means clustering algorithm was used to divide contiguous time steps with similar active power load into groups, where one adjustment per device is permitted within each cluster.

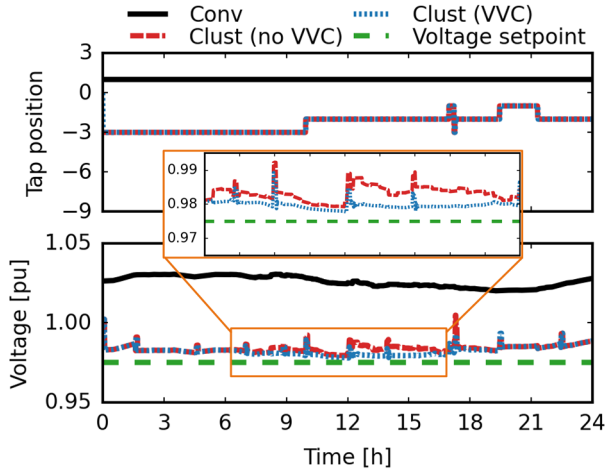


Fig. 5. Substation transformer LTC settings (top) and system PCC voltage (bottom) for the three control cases. The clust (VVC) case maintained PCC voltage closer to the target voltage in-between utility device adjustments due to the quicker response time of SIs.

An optimization with minimization objectives of system active power and voltage violations was implemented using a Non-dominated Sorting Genetic Algorithm (NSGA) to determine optimal device settings for each cluster. A more detailed description of the cluster-based method is included in a previous publication by our group [21].

To further improve system response time to sudden voltage fluctuations in distribution grids with high DER penetration, a new multi-timescale approach for combined voltage and reactive power control of utility devices and SIs is proposed. In this new combined two-method control, switching operations of CBs and LTCs are dispersed over time with the cluster-based method while faster responses are implemented with SI VVC, as shown in Fig. 4. This method increases grid resilience by complementing the weakness of mechanical switching devices, which are limited in allowed adjustments to preserve equipment lifetime, with electronic SI control to allow for quicker response to voltage fluctuations in distribution grids with highly variable renewable generation.

V. CASE STUDY: MULTI-TIMESCALE VOLTAGE AND REACTIVE POWER CONTROL OF UTILITY DEVICES AND SIs

Three cases were simulated on the KUsIT1 circuit: conventional control (conv), cluster-based control without SI VVC (clust (no VVC)), and cluster-based control with SI VVC (clust (VVC)). Conv implements a traditional approach where CBs are always “ON” and the substation transformer LTC remains at the “1” position unless system voltage is outside the acceptable margin. The conv case represents a system without advanced control to serve as the baseline for comparison. Clust (no VVC) implements cluster-based control of CBs and the transformer LTC without SI VVC.

Finally, clust (VVC) implements multi-timescale control of utility devices and SIs where switching operations are

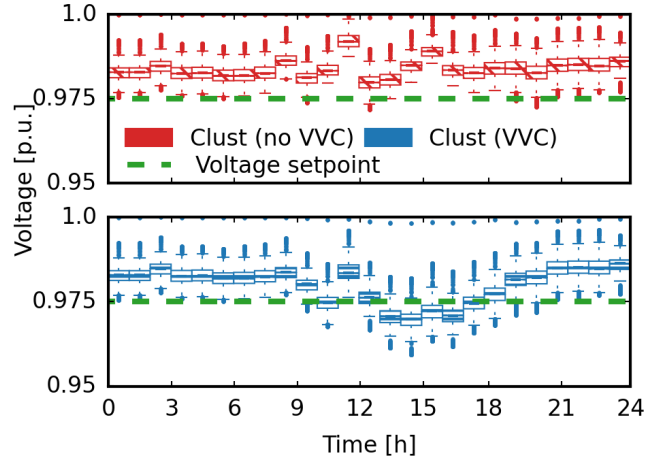


Fig. 6. System node voltages for the clust (no VVC) case (top) and the clust (VVC) case (bottom). Clust (VVC) maintained system voltage closer to the voltage setpoint, especially during times of high solar PV generation. There were no recorded voltage violations (<0.95 or >1.05 pu) at any node during the 24-hour simulation.

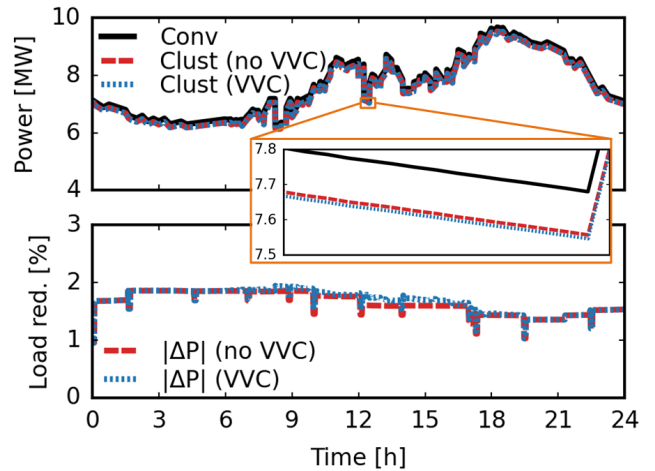


Fig. 7. Total system active power load (top) and percent load reduction in comparison to the conventional control case (bottom). In the clust (VVC) case, load reduction due to CVR was higher midday when PV generation was high, since more reactive power could be absorbed to decrease voltage.

cluster-based and SI VVC settings can be adjusted on a per-minute basis. Voltage setpoints V_1 , V_2 , V_3 and V_4 for SI VVC were set to 0.95, 0.96, 0.975, and 0.99pu respectively to represent an example combined control case. All SIs calculate reactive power injection/absorption based on voltage at the PCC, i.e. the substation transformer, for each timestep. In the advanced control cases, the target voltage was set to 0.975pu to implement CVR while also ensuring node voltage did not fall below 0.95pu due to voltage drop between the substation and loads.

VI. RESULTS AND DISCUSSION

Voltages at the PCC and LTC tap positions for all three cases are shown in Fig. 5. During hours of high solar PV

TABLE I
SIMULATION RESULTS OF THE THREE CONSIDERED CONTROL CASES

System Power Flow	Conv	Clust (no VVC)	Clust (VVC)
Tot. Energy [MWh]	183.68	180.69	180.63
Energy Red. [%]	-	1.63	1.66
Tot. Losses [MWh]	2.19	1.69	1.68
Peak Act. Pwr. [MW]	9.67	9.53	9.52
Peak Reac. Pwr. [MVAR]	1.82	1.75	2.18
Grid Operation	Conv	Clust (no VVC)	Clust (VVC)
Tot. Volt. Viol.	0	0	0
Tot. No. of LTC Adjmts.	0	7	7
Tot. No. of CB Adjmts.	0	35	35

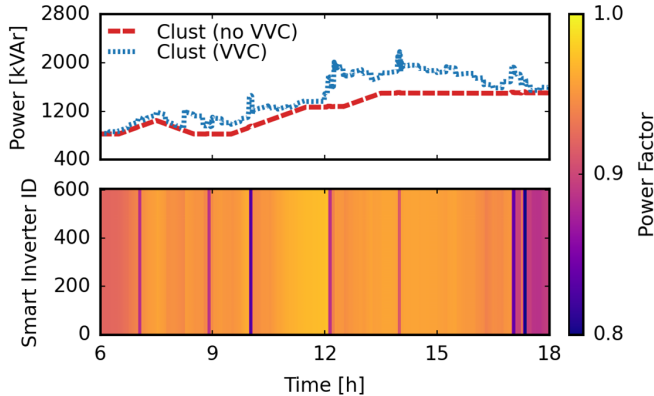


Fig. 8. System reactive power load for the cluster-based control cases (top) and selected PF settings for SIs in the clust (VVC) case during solar generation hours. In the clust (VVC) case, SIs used surplus capacity to absorb VARs, which decreased PCC voltage closer to the target voltage setpoint.

generation, system voltage was kept closer to the target voltage in-between utility device adjustments in the clust (VVC) case due to the quicker response time of SI VVC. During the 24-hour simulation, there were no voltage violations (<0.95 or >1.05 pu) at any node in the system as expected and required. This is illustrated in the box plot of distribution system node voltages in Fig. 6.

Additionally, both advanced control cases maintained satisfactory CVR active power load reduction from the conv case between 1 to 2%, with the clust (VVC) case outperforming the clust (no VVC) case during midday when solar PV generation was high, as shown in Fig. 7. Total CVR energy reduction from the conv case was 1.63% and 1.66% for the clust (no VVC) and clust (VVC) cases respectively, as listed in the results from Tab. I. This energy reduction with the same number of utility device adjustments was achieved by the clust (VVC) case with example VVC voltage setpoints and the same PF setting for all SIs at each timestep. As shown in Fig. 8, for each time step the same PF setting was selected for all SIs in the system, which caused sudden changes in reactive power, especially when solar PV generation was high. Results may be further improved with decentralized control methods to vary voltage setpoints and reactive power output for SIs at different locations in the distribution grid.

VII. CONCLUSION

Extensive experimental and synthetically-generated data was used to perform voltage and reactive power optimization on a DT of a real, very large distribution system with 2,018 nodes and 8.65MW peak load. The proposed multi-timescale cluster-based VVC method was tested against baseline control cases to evaluate its performance under high volatility caused by high DER penetration. This method dispersed utility device operations while allowing fast response with SIs to complement their limitations.

The proposed method limited total CB and LTC adjustments to within the equipment degradation reduction range, i.e. 35 and 7 respectively over a 24-hour period. Concurrently, SIs were dispatched for reactive power support in-between switching operations. Total energy savings of 1.66% were achieved in comparison to traditional utility conventional control with zero system voltage violations. Assuming similar savings per day, estimated energy savings for the simulated circuit alone were over 1,100MWh annually.

ACKNOWLEDGMENT

This paper is based upon work supported by the National Science Foundation (NSF) under NSF Graduate Research Fellowship Grant No. 2239063. The support of PPL Corporation, the Lighthouse Beacon Foundation and L. Stanley Pigman Chair in Power Endowment at University of Kentucky are also gratefully acknowledged. Any opinions, findings, and conclusions, or recommendations expressed in this material are those of the authors and do not necessarily reflect the views of the sponsoring organizations.

REFERENCES

- [1] A. Savasci, A. Inaolaji, and S. Paudyal, "Two-stage volt-var optimization of distribution grids with smart inverters and legacy devices," *IEEE Transactions on Industry Applications*, vol. 58, no. 5, pp. 5711–5723, 2022.
- [2] F. Blaabjerg and D. M. Ionel, *Renewable energy devices and systems with simulations in MATLAB® and ANSYS®*. Boca Raton, FL: CRC Press, 2017.
- [3] IEEE Standards Coordinating Committee 21, "IEEE standard for interconnection and interoperability of distributed energy resources with associated electric power systems interfaces," *IEEE Std 1547-2018 (Revision of IEEE Std 1547-2003)*, pp. 1–138, 2018.
- [4] M. A. Hasan, N. K. Vemula, R. Devarapalli, and Ł. Knypiński, "Investigation into PV inverter topologies from the standards compliance viewpoint," *Energies*, vol. 17, no. 16, p. 3879, 2024.
- [5] M. Zhang, Q. Xu, S. Magnússon, R. C. Pilawa-Podgurski, and G. Guo, "Multi-agent deep reinforcement learning for decentralized voltage-var control in distribution power system," in *2022 IEEE ECCE*. IEEE, 2022, pp. 1–5.
- [6] F. Liu and Q. Xu, "Safe deep reinforcement learning based volt-var control for three-phase unbalanced distribution system with PV integration," in *2024 IEEE ECCE*. IEEE, 2024, pp. 1823–1828.
- [7] R. Yan, Q. Xing, and Y. Xu, "Multi-agent safe graph reinforcement learning for PV inverters-based real-time decentralized volt/var control in zoned distribution networks," *IEEE Transactions on Smart Grid*, vol. 15, no. 1, pp. 299–311, 2023.
- [8] R. R. Jha, S. Poudel, P. Sharma, A. Dubey, and K. P. Schneider, "Volt/var optimization (vvo) application on gridapps-d platform," in *2023 IEEE PESGM*. IEEE, 2023, pp. 1–5.

- [9] B. Zhu, L. Wu, Y. Xiao, R. Diao, and F. Sun, "Supervised learning-aided volt/var control for active distribution networks with increasing renewable energy considering uncertainties," in *2023 4th International Conference on Advanced Electrical and Energy Systems (AEES)*. IEEE, 2023, pp. 535–539.
- [10] H. Li and R. ElShatshat, "Optimal reinforcement learning-based double-layer volt/var control for active distribution systems," in *2024 IEEE Power & Energy Society General Meeting (PESGM)*, 2024, pp. 1–5.
- [11] S. Singh, S. Veda, S. P. Singh, R. Jain, and M. Baggu, "Event-driven predictive approach for real-time volt/var control with cvr in solar PV rich active distribution network," *IEEE Transactions on Power Systems*, vol. 36, no. 5, pp. 3849–3864, 2021.
- [12] M. McNamara, D. Feng, T. Pettit, and D. Lawlor, "Conservation Voltage Reduction/Volt VAR Optimization EM&V Practices," United States Environmental Protection Agency, Tech. Rep., January 2017. [Online]. Available: <https://www.energystar.gov/products/productstr>
- [13] Z. Wang and J. Wang, "Review on implementation and assessment of conservation voltage reduction," *IEEE Transactions on Power Systems*, vol. 29, no. 3, pp. 1306–1315, 2013.
- [14] K. P. Schneider, J. C. Fuller, F. K. Tuffner, and R. Singh, "Evaluation of conservation voltage reduction (CVR) on a national level," Pacific Northwest National Lab.(PNNL), Richland, WA (United States), Tech. Rep., 2010.
- [15] E. S. Jones, N. Jewell, Y. Liao, and D. M. Ionel, "Optimal capacitor placement and rating for large-scale utility power distribution systems employing load-tap-changing transformer control," *IEEE Access*, vol. 11, pp. 19 324–19 338, 2023.
- [16] E. P. R. I. (EPRI), "DOE SHINES Residential Demonstration," available: <https://dashboards.epri.com/shines-residential>.
- [17] U. S. D. of Transportation, "National Household Travel Survey," 2017, available: <https://nhts.ornl.gov/>.
- [18] CBEECC-Res Compliance Software Project, "CBEECC-Res 2019," 2019, <http://www.bwilcox.com/BEES/cbecc2019.html>.
- [19] S. B. Poore, R. E. Alden, T. Rooney, and D. M. Ionel, "New loads and service factors for distribution transformers following the transition to high-efficiency heat pumps, solar PV, and ev charging," in *2024 IEEE Energy Conversion Congress and Exposition (ECCE)*. IEEE, 2024, pp. 1031–1036.
- [20] sunwatts, "7.7kW SMA Sunny Boy Smart Energy Hybrid Inverter," <https://sunwatts.com/7-7kw-sma-sunny-boy-smart-energy-hybrid-inverter/>, Accessed: July 17th, 2025.
- [21] S. B. Poore, G. M. Fischer, R. E. Alden, E. S. Jones, A. Patrick, and D. M. Ionel, "Cluster-based volt/var optimization on a utility distribution feeder with forecasted ev penetration," in *2025 IEEE Transportation Electrification Conference (ITEC)*. IEEE, 2025.